PROCEEDINGS, 43rd Workshop on Geothermal Reservoir Engineering
Stanford University, Stanford, California, February 12-14, 2018
SGP-TR-213

Imaging Fracture Zones Using Continuous Active Source Seismic Monitoring for the EGS Collab Project: A Synthetic Study

Kai Gao[a], Lianjie Huang[a], Benxin Chi[a], Jonathan Ajo-Franklin[b] and EGS Collab Team[1]

[a]Geophysics Group, Los Alamos National Laboratory, Los Alamos, NM 87544

[b]Geophysics Department, Lawrence Berkeley National Laboratory, Berkeley, CA 94720

kaigao@lanl.gov; ljh@lanl.gov; benxinchi@lanl.gov; jbajo-franklin@lbl.gov

Keywords: anisotropic medium, continuous active source seismic monitoring, enhanced geothermal system, fracture zone, full-waveform inversion, reverse-time migration.

ABSTRACT

The EGS Collab project of the U.S. Department of Energy is conducting a field experiment at the Stanford Underground Research Facility (SURF) site to study subsurface fracture creation and appropriate tools for characterization and monitoring. The SURF site is located in Lead, South Dakota, at the site of the former Homestake Gold Mine. The EGS Collab project is conducting the experiment from a drift located approximately 1.5 km beneath the surface. A multi-level continuous active source seismic monitoring (ML-CASSM) system designed by Lawrence Berkeley National Laboratory will be used to monitor fracture creation, coupled to extensive passive (microseismic) monitoring. Four fracture-parallel boreholes and two orthogonal boreholes will be used to acquire active and passive seismic data during the experiment. We use the same borehole configuration and geophone distribution to conduct a numerical study in order to evaluate the potential to image the created fracture. We perform anisotropic elastic full-waveform inversion of synthetic transmission and reflection data to image the fracture. To alleviate artifacts caused by sparse seismic data, we employ high-order compressive sensing in our anisotropic elastic full-waveform inversion. Our results demonstrate that it is possible to use the ML-CASSM system to image the fracture created during the EGS Collab experiment.

1. INTRODUCTION

Fracture characterization is essential for many geothermal applications. For instance, hydraulic stimulation is usually used in enhanced geothermal systems (EGS) to create fractures for heat exchange with a working fluid. Accurate fracture imaging and physical property estimation is therefore an indispensable procedure to provide essential information about the effectiveness of enhanced geothermal systems. Geophysical monitoring is a key component for the EGS Collab (Stimulation Investigations for Geothermal Modeling Analysis and Validation) project initiated and supported by the US DOE Geothermal Technologies Office (GTO) (Dobson et al., 2017; Kneafsey et al., 2018). The EGS Collab project is conducting a field experiment at the Stanford Underground Research Facility (SURF) site to study fracture creation and imaging. The SURF site is located in Lead, South Dakota, at the former site of the Homestake Gold Mine. The EGS Collab project is conducting the experiment from a drift located approximately 1.5 km beneath the surface. A multi-level continuous active source seismic monitoring (ML-CASSM) system designed by Lawrence Berkeley National Laboratory (Ajo-Franklin *et al*., 2011; Daley *et al*., 2011; Huang *et al*., 2017) will be used to monitor the fractures created by hydraulic stimulations. The ML-CASSM approach involves the deployment of spatially fixed and highly automated seismic source and receiver arrays. Removing the need for manual repositioning of equipment increases temporal resolution and improves repeatability, allowing the detection of subtle property variations. Four fracture-parallel boreholes and two fracture-orthogonal boreholes are used to acquire active and passive seismic data during the experiment (Figure 1).

Our numerical study uses the experimental borehole configuration and sensor distribution to evaluate the potential to image the created fractures. We perform anisotropic elastic-waveform inversion of synthetic transmission and reflection data to image the fractures. We also study the influence of the numbers of sources and geophones on the inversion quality of the fracture locations and properties. Sparse source/geophone distribution usually leads to poor-quality inversion and imaging results. To reduce the artifacts caused by sparse seismic data, we employ a high-order compressive-sensing regularization scheme in our anisotropic elastic-waveform inversion (AEWI) to reduce

[1]J. Ajo-Franklin, S.J. Bauer, T. Baumgartner, K. Beckers, D. Blankenship, A. Bonneville, L. Boyd, S.T. Brown, J.A. Burghardt, T. Chen, Y. Chen, C. Condon, P.J. Cook, P.F. Dobson, T. Doe, C.A. Doughty, D. Elsworth, J. Feldman, A. Foris, L.P. Frash, Z. Frone, P. Fu, K. Gao, A. Ghassemi, H. Gudmundsdottir, Y. Guglielmi, G. Guthrie, B. Haimson, A. Hawkins, J. Heise, C.G. Herrick, M. Horn, R.N. Horne, J. Horner, M. Hu, H. Huang, L. Huang, K. Im, M. Ingraham, T.C. Johnson, B. Johnston, S. Karra, K. Kim, D.K. King, T. Kneafsey, H. Knox, J. Knox, D. Kumar, K. Kutun, M. Lee, K. Li, R. Lopez, M. Maceira, N. Makedonska, C. Marone, E. Mattson, M.W. McClure, J. McLennan, T. McLing, R.J. Mellors, E. Metcalfe, J. Miskimins, J.P. Morris, S. Nakagawa, G. Neupane, G. Newman, A. Nieto, C.M. Oldenburg, W. Pan, R. Pawar, P. Petrov, B. Pietzyk, R. Podgorney, Y. Polsky, S. Porse, S. Richard, M. Robertson, B. Roggenthen J. Rutqvist, H. Santos-Villalobos, P. Schwering, V. Sesetty, A. Singh, M.M. Smith, H. Sone, C.E. Strickland, J. Su, C. Ulrich, A. Vachaparampil ,C.A. Valladao, W. Vandermeer, G. Vandine, D. Vardiman, V.R.. Vermeul, J.L. Wagoner, H.F. Wang, J. Weers, J. White, M.D. White, P. Winterfeld Y.S. Wu, Y. Wu, Y. Zhang, Y.Q. Zhang, J. Zhou, Q. Zhou, M.D. Zoback

artifacts and improve convergence of inversion. Our numerical results demonstrate that it is possible to use sparse ML-CASSM systems to image the fractures created during the EGS Collab experiment.

We first briefly introduce the formulations of our anisotropic elastic-waveform inversion algorithm, describe the configuration of the active seismic sources and receivers used in our numerical study for the EGS Collab project, and then present our AEWI results based on ML-CASSM configurations with different numbers of sources and geophones.

2. METHODOLOGY

To estimate anisotropic elastic properties of subsurface media, we use anisotropic elastic-waveform inversion to invert for elasticity parameters C_{ij} $(i,j = 1,2,\dots,6)$. Our AEWI algorithm is based on the elastic-wave equation in the following first-order form:

$$\rho \frac{\partial v}{\partial t} = \Lambda\sigma + f, \tag{1}$$

$$\frac{\partial \sigma}{\partial t} = C\Lambda^T v, \tag{2}$$

where $v = (v_x, v_y, v_z)$ is the particle velocity wavefield, $\sigma = (\sigma_{xx}, \sigma_{yy}, \sigma_{zz}, \sigma_{yz}, \sigma_{xz}, \sigma_{xy})$ is the stress wavefield, Λ is a differential operator (Vigh *et al*., 2014), ρ is the density of the media, and $C = C_{ij}$ is the elasticity matrix of the medium.

AEWI attempts to minimize the misfit function between the synthetic data $f(m)$ and the observed data d:

$$\chi(m) = \sum_{N_s,N_r} \int_0^T [d - f(m)]^2 dt\ , \tag{3}$$

where N_s and N_r represent the number of sources and geophones in the monitoring/imaging system, respectively. For field data applications, matching wavefield amplitudes using equation (3) is usually difficult and can easily lead to convergence to a local minimum of the misfit function. We employ a correlation-type misfit function (Choi and Alkhalifah, 2016) to alleviate this problem.

We update elasticity parameters, C_{ij}, using the gradients computed based on the cross-correlation between the source wavefield and the back-propagated adjoint wavefield. The full expressions for computing these gradients can be found in Vigh *et al*. (2014). For instance, the gradient of the misfit function $\chi(m)$ w.r.t. the elasticity parameter C_{11} reads:

$$\frac{\partial \chi}{\partial C_{11}} = -\sum_{N_s,N_r} \int_0^T \varepsilon_{11}\varepsilon_{11}^{\dagger} dt\ , \tag{4}$$

where ε is the source strain wavefield, and the superscript "†" represents the adjoint strain wavefield. The strain wavefields can be obtained from combining the elastic compliance and the stress wavefield based on Hooke's law. The gradients of the misfit function w.r.t. other parameters can be derived similarly.

We test different parameterizations in AEWI, and find that the velocity parameterization can provide improved flexibility and convergence for ML-CASSM fracture characterization. The velocity update can be computed conveniently with the chain rule of differentiation. For instance, to update the P-wave velocity, we use

$$\frac{\partial \chi}{\partial V_p} = \sum_{i,j} \frac{\partial \chi}{\partial C_{ij}} \frac{\partial C_{ij}}{\partial V_p}. \tag{5}$$

During inversion, we use different step lengths for different inversion parameters in the optimal step size search to provide maximal flexibility. Existing AEWI techniques usually assume the same step size for different parameters (e.g., Vigh *et al*., 2014).

The source/geophone distribution in the ML-CASSM data acquisition is often sparse during experiments because of the high cost of fabricating multi source arrays. Therefore, we developed an AEWI method with a high-order compressing-sensing (HOCS) regularization scheme to reduce inversion artifacts and improve inversion robustness for sparse data. In our HOCS-AEWI, the misfit function is defined as

$$\chi_{HOCS}(m) = \sum_{N_s,N_r} \int_0^T [d - f(m)]^2 dt\ + \alpha_1 \|\nabla m - w\|_p + \alpha_1 \|\varepsilon(w)\|_p, \tag{6}$$

where $\varepsilon(w)$ is a mixed matrix term for holding the second-order mono-directional and mixed spatial derivatives of auxiliary variable w, and p is the norm that controls the sparsity-promoting degree of AEWI. Usually, $p = 0.5$ provides the superior performance. The inversion problem based on equation (6) can be solved with the split Bregman decomposition framework (Lin and Huang, 2014).

3. RESULTS

We conduct synthetic study of ML-CASSM for characterizing fractures to be created at SURF under the EGS Collab project. Figure 1 is a schematic illustration of the EGS Collab experiment and ML-CASSM configuration at SURF. ML-CASSM sources and sensors are installed in four parallel wells as shown in Figure 1. The EGS Collab Experiment 1 plans to create two parallel fractures using hydraulic stimulation. The two fractures are located between the two sets of parallel wells, each with a radius of 10 m. The injection well is perpendicular to the fracture surfaces and penetrates through the center of the two fractures. The production well is also perpendicular to

the fracture surfaces by separated 10 m away from the injection well. The ML-CASSM sources/geophones are placed around the centers of the four parallel monitoring wells near the fractures.

We assume the rock is a vertical transverse isotropic (VTI) medium and the anisotropy symmetry axis is parallel with the fracture surfaces.

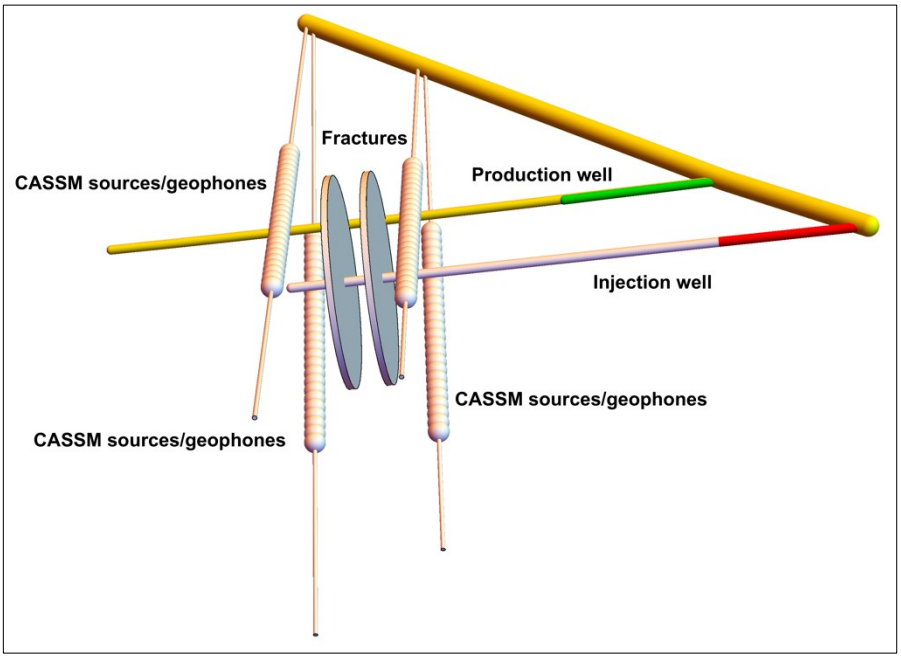

Figure 1: A sketch of the EGS Collab experiment and ML-CASSM configuration for characterizing two fractures created by hydraulic stimulation. The two fractures are parallel in space, and are perpendicular to the injection and production wells. Locations and lengths of the wells are based on real borehole configurations.

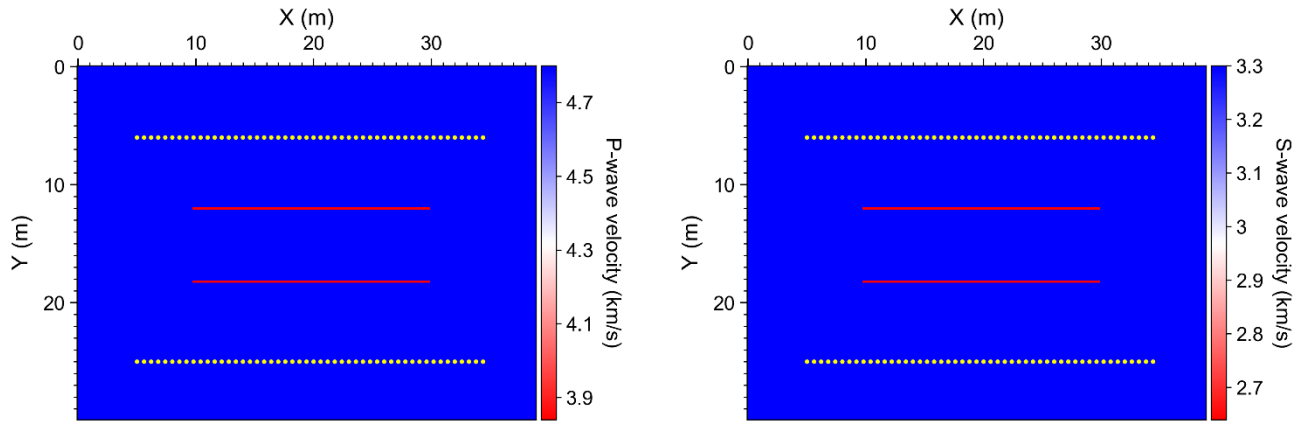

(a) (b)

Figure 2: (a) The true P-wave velocity model and (b) the true S-wave velocity model. The two red lines represent the two parallel fractures. Yellow dots represent the locations of ML-CASSM sources or geophones. The initial models for AEWI are set to be homogeneous.

The frequency spectrum of the source emission in realistic ML-CASSM experiments is fairly wide, ranging from approximately 500 Hz to 5,000 Hz. To provide sufficient resolution in the AEWI tests shown below, we assume that the source emission has a Ricker wavelet temporal signature, with a central frequency of 3,000 Hz.

We conduct a series of numerical AEWI experiments using both synthetic transmission and reflection data to demonstrate the feasibility of different ML-CASSM configurations for detecting and characterizing fractures between the parallel monitoring wells. Our numerical

tests are all for noise-free synthetic data. To simplify the numerical tests, we extract a representative horizontal slice from the 3D model shown in Figure 1. The extracted 2D slice is shown in Figure 2, with the true P- and S-wave velocity modes in Figure 2(a) and 2(b), respectively.

We conduct AEWI to investigate if we can reconstruct the locations and medium properties (P- and S-wave velocities) of these two fractures using a certain number of sources/geophones. In the AEWI tests, we use homogeneous models as the initial models, resembling the fact that in practice we have no knowledge of the locations or medium properties of fractures before imaging or inversion using acquired ML-CASSM data.

We first conduct an AEWI test using a total of 50 sources, with 25 sources on each side of the fractures, as shown in Figure 3. In addition, we use a total of 100 geophones, with 50 geophones on each side of the fractures. The locations of the sources and geophones are shown using the yellow dots and red star marks in Figure 3.

Our reconstructed P- and S-wave velocity models are shown in Figures 3(a) and 3(b), respectively. It is evident that our AEWI can accurately reconstruct the locations and medium properties of the two fractures, starting from homogeneous initial models. The final data misfit after 40 iterations in this numerical test is less than 0.05% of the initial data misfit.

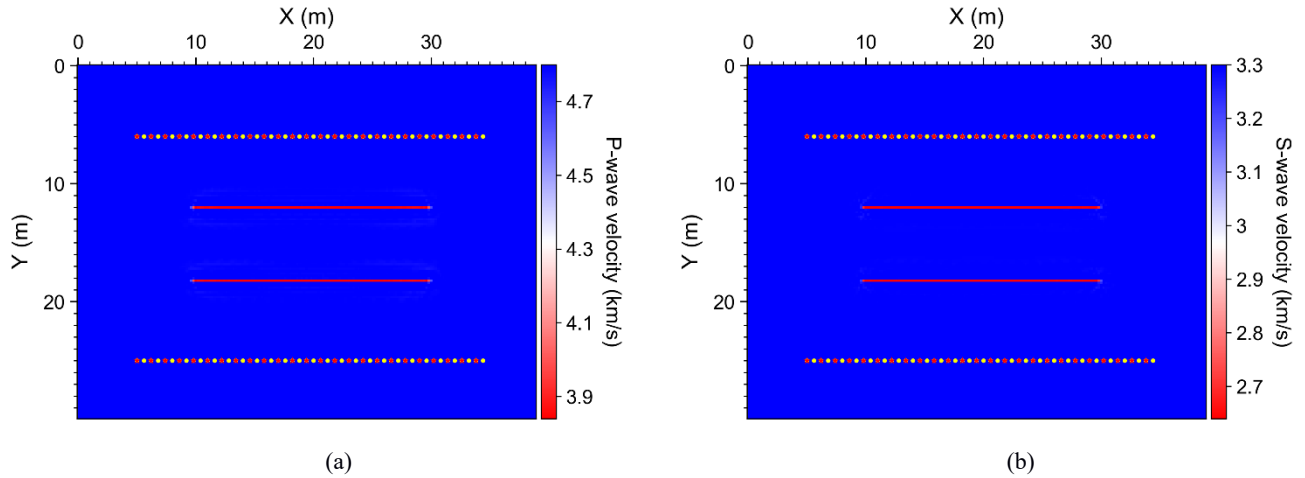

(a) (b)

Figure 3: (a) The inverted P-wave velocity model and (b) the inverted S-wave velocity model obtained using the conventional AEWI without regularization. Yellow dots represent the locations of ML-CASSM geophones, and red stars between the yellow dots represent the locations of ML-CASSM sources. We use a total of 50 sources and 100 geophones in this numerical test. One half of the number of sources and geophones are on each side of the two fractures.

We conduct numerical studies to determine the minimum numbers of sources/geophones needed to reconstruct the fracture locations and properties in the framework of ML-CASSM. We first use 12 sources/geophones on each side of the fractures, and employ our HOCS-AEWI to invert for the fracture locations and properties. The final data misfit is less than 0.03% of the initial data misfit. The reconstructed fractures are shown in Figure 4. The reconstructed velocity models are visibly identical to the results in Figure 3, which are produced using the geometry of 50 sources and 100 geophones. Clearly, a total of 24 sources/geophones is adequate to provide a fairly good reconstruction of the fractures.

We then use 6 sources on each side of the fractures, and use our HOCS-AEWI to estimate the fracture locations and properties. The reconstructed fractures are shown in Figure 5. In this case, the boundaries of the two fractures are well reconstructed. However, the P- (Figure 5a) and S-wave velocities (Figure 5b) of the fractures are reconstructed with visible inaccuracy, particularly on the ends of the two fractures. The deviations result from the fact that there are too few sources/geophones in the acquisition system and the data coverage for fracture imaging is poor.

In the last numerical test, we use only three sources and three geophones on each side of the fractures, and depict the AEWI reconstruction of the P- and S-wave velocity models in Figure 6(a) and 6(b), respectively. The results are even less accurate compared to those in Figure 5 obtained using six sources and six geophones on each side of the fractures. In this case, because the geometry is too sparse, we can observe some discontinuities and other artifacts in the reconstructed fractures.

These numerical tests show that we can accurately estimate the fracture location and medium property using the ML-CASSM configuration during the EGS Collab experiment. Specifically, we can use a total of 24 sources/geophones to well reconstruct the medium properties and the locations of the two fractures using our HOCS-AEWI. Using fewer sources/geophones can produce a satisfactory reconstruction of the locations of fractures, yet the estimated medium properties can deviate from the true values. Our numerical studies demonstrate that at least a total of 12 source/geophones (6 on each side of the fractures) is needed to reliably reconstruct fracture locations and properties for the EGS Collab experiment.

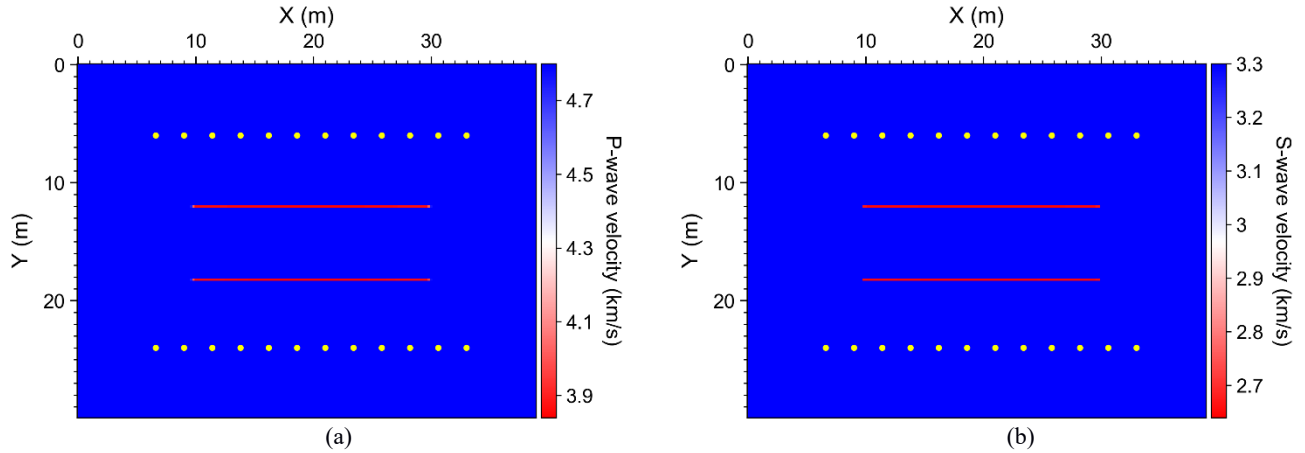

Figure 4: (a) The inverted P-wave velocity model and (b) the inverted S-wave velocity model obtained using HOCS-AEWI. Yellow dots represent the locations of ML-CASSM sources/geophones. We use a total of 24 sources/geophones (12 on each side of the two fractures) in this numerical test.

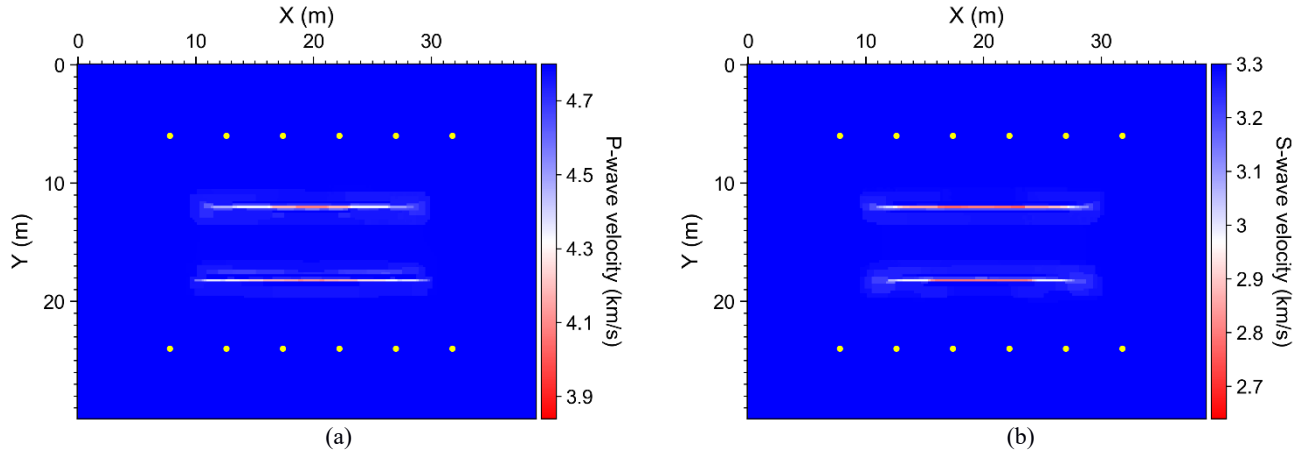

Figure 5: (a) The inverted P-wave velocity model and (b) the inverted S-wave velocity model obtained using HOCS-AEWI. Yellow dots represent the locations of ML-CASSM sources/geophones. We use a total of 12 sources/geophones (6 on each side of the two fractures) in this numerical test.

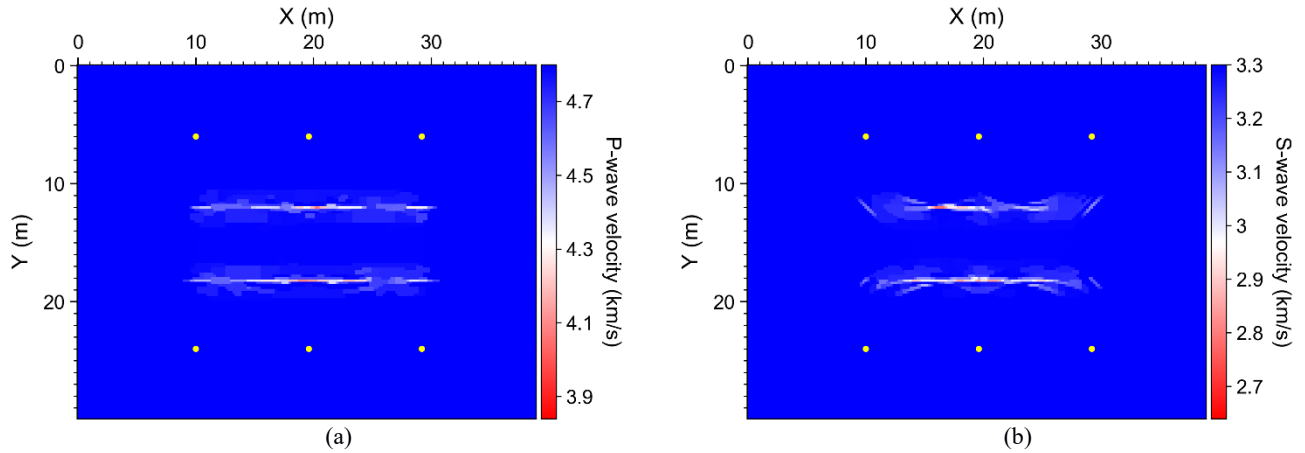

Figure 6: (a) The inverted P-wave velocity model and (b) the inverted S-wave velocity model obtained using HOCS-AEWI. Yellow dots represent the locations of ML-CASSM sources/geophones. We use a total of 6 sources/geophones (3 on each side of the two fractures) in this numerical test.

4. CONCLUSIONS

We have conducted anisotropic elastic-waveform inversion to study the feasibility of estimating locations and properties of the two fractures using ML-CASSM in the EGS Collab experiment. Our numerical experiments show that it is possible to accurately reconstruct the locations and properties of fractures using a total of 24 sources and geophones. Fewer sources and geophones can delineate the locations of fractures, yet the estimated medium property values deviate from the true values. Using high-order compressive-sensing regularization in anisotropic elastic full-waveform inversion can alleviate inversion inaccuracy caused by sparse source/receiver geometry. We find that, under the source frequency and medium parameter settings used in our synthetic numerical study, an ML-CASSM configuration with at least a total of approximately six sources and geophones is needed for our anisotropic elastic-waveform inversion to accurately and reliably reconstruct the locations and properties of subsurface fractures. In practice, more than six sources/geophones are needed because of noisy data.

5. ACKNOWLEDGMENTS

This material was based upon work supported by the U.S. Department of Energy, Office of Energy Efficiency and Renewable Energy (EERE), Office of Technology Development, Geothermal Technologies Office, under Award Number DE-AC52-06NA25396 to Los Alamos National Laboratory (LANL) and Award Number DE-AC02-05CH11231 with Lawrence Berkeley National Laboratory (LBNL). We thank Timothy Kneafsey of LBNL for his careful review of the paper. The United States Government retains, and the publisher, by accepting the article for publication, acknowledges that the United States Government retains a non-exclusive, paid-up, irrevocable, world-wide license to publish or reproduce the published form of this manuscript, or allow others to do so, for United States Government purposes. The computation was performed using super-computers of LANL's Institutional Computing Program.

REFERENCES

Ajo-Franklin, J.B., Daley, T.M., Butler-Veytia, B., Peterson, J., Wu, Y., Kelley, B., and Hubbard, S.: Multi-level continuous active source seismic monitoring (ML-CASSM): Mapping shallow hydrofracture evolution at a TCE contaminated site, *Extended Abstracts of Society of Exploration Geophysicists Annual Meeting*, (2011).

Choi, Y., and Alkhalifah, T.: An optimized correlation-based full waveform inversion, *78th EAGE Conference and Exhibition*, Vienna, Austria (2016).

Daley, T., Ajo-Franklin, J.B., and Doughty, C.: Constraining the reservoir model of an injected CO_2 plume with crosswell ML-CASSM at the Frio-II Brine Pilot, *International Journal of Greenhouse Gas Control*, **5**, 2, (2011), 1022-1030.

Dobson, P., Kneafsey, T.J., Blankenship, D., Valladao, C., Morris, J., Knox, H., Schwering, P., White, M., Doe, T., Roggenthen, W., Mattson, E., Podgorney, R., Johnson, T., Ajo-Franklin, J., and EGS Collab Team, "An Introduction to the EGS Collab SIGMA-V Project: Stimulation Investigations for Geothermal Modeling Analysis and Validation," GRC Transactions, 41, (2017), 837-849.

Huang, L., Chen, Y., Gao, K., Fu, P., Morris, J., Ajo-Franklin, J., Nakagawa, S., EGS Collab Team: Numerical modeling of seismic and displacement-based monitoring for the EGS Collab Project, *GRC Transactions*, **41**, (2017).

Kneafsey, T.J., Dobson, P., Blankenship, D., Morris, J., Knox, H., Schwering, P., White, M., Doe, T., Roggenthen, W., Mattson, E., Podgorney, R., Johnson, T., Ajo-Franklin, J., Valladao, C., and the EGS Collab team: An Overview of the EGS Collab Project: Field Validation of Coupled Process Modeling of Fracturing and Fluid Flow at the Sanford Underground Research Facility, Lead, SD, *PROCEEDINGS*, 43rd Workshop on Geothermal Reservoir Engineering, Stanford University, Stanford, California, SGP-TR-213 (2018).

Lin, Y., and Huang, L.: Acoustic- and elastic-waveform inversion using a modified total-variation regularization scheme: *Geophysical Journal International*, **200**, (2014), 489–502.

Vigh, D., Jiao, K., Watts, D., and Sun, D.: Elastic full-waveform inversion application using multicomponent measurements of seismic data collection: *Geophysics*, **79**, (2014), R63–R77.